3-10-2023

Disturbances in primary visual processing as a function of healthy aging

Seth D. Springer

Tara D. Erker

Mikki Schantell

Hallie J. Johnson

Madelyn P. Willett

See next page for additional authors

Authors

Seth D. Springer, Tara D. Erker, Mikki Schantell, Hallie J. Johnson, Madelyn P. Willett, Hannah J. Okelberry, Maggie P. Rempe, and Anthony Wilson

NeuroImage 271 (2023) 120020

Contents lists available at ScienceDirect

NeuroImage

journal homepage: www.elsevier.com/locate/neuroimage

Disturbances in primary visual processing as a function of healthy aging

Seth D. Springer[a,b], Tara D. Erker[a,c], Mikki Schantell[a,b], Hallie J. Johnson[a], Madelyn P. Willett[a], Hannah J. Okelberry[a], Maggie P. Rempe[a,b], Tony W. Wilson[a,b,d,*]

[a] Institute for Human Neuroscience, Boys Town National Research Hospital, Boys Town, NE, USA
[b] College of Medicine, University of Nebraska Medical Center, Omaha, NE, USA
[c] College of Engineering, University of Nebraska – Lincoln, Lincoln, NE, USA
[d] Department of Pharmacology & Neuroscience, Creighton University, Omaha, NE, USA

ARTICLE INFO

Keywords:
Cortical entrainment
Visual flicker
Alpha
Ageing
Cortical thickness
Oscillatory
Phase-locked
Harmonics

ABSTRACT

For decades, visual entrainment paradigms have been widely used to investigate basic visual processing in healthy individuals and those with neurological disorders. While healthy aging is known to be associated with alterations in visual processing, whether this extends to visual entrainment responses and the precise cortical regions involved is not fully understood. Such knowledge is imperative given the recent surge in interest surrounding the use of flicker stimulation and entrainment in the context of identifying and treating Alzheimer's disease (AD). In the current study, we examined visual entrainment in eighty healthy aging adults using magnetoencephalography (MEG) and a 15 Hz entrainment paradigm, while controlling for age-related cortical thinning. MEG data were imaged using a time-frequency resolved beamformer and peak voxel time series were extracted to quantify the oscillatory dynamics underlying the processing of the visual flicker stimuli. We found that, as age increased, the mean amplitude of entrainment responses decreased and the latency of these responses increased. However, there was no effect of age on the trial-to-trial consistency in phase (i.e., inter-trial phase locking) nor amplitude (i.e., coefficient of variation) of these visual responses. Importantly, we discovered that the relationship between age and response amplitude was fully mediated by the latency of visual processing. These results indicate that aging is associated with robust changes in the latency and amplitude of visual entrainment responses within regions surrounding the calcarine fissure, which should be considered in studies examining neurological disorders such as AD and other conditions associated with increased age.

1. Introduction

Aging, even in the absence of pathological changes, has been shown to affect a variety of visual processes, including visual acuity (Elliott et al., 1995), motion perception (Trick and Silverman, 1991), and contrast sensitivity (Burton et al., 1993; Elliott et al., 1990). These changes in visual processing during healthy aging are the result of complex and multifaceted alterations along the entire visual pathway; from the cornea to the visual cortices (Erdinest et al., 2021). Understanding the nature of visual processing deficits in aging is critical considering that decrements in basic visual processing have been shown to significantly decrease the quality of life of older adults (Brenner et al., 1993) and can lead to increased risk of injury (e.g., via falling or accidents while driving; Lord et al., 2002; Owsley et al., 1998; Sakai et al., 2015).

A common neurological change associated with healthy aging is the gradual decrease of cortical thickness across the whole brain (Fjell et al., 2009; Frangou et al., 2021). Though general age-related decreases in cortical thickness have been commonly reported, analyses tend to show less occipital cortical thinning relative to other cortical areas (Allen et al., 2005; Griffis et al., 2016; Raz et al., 2004; Salat et al., 2004; Thambisetty et al., 2010). Importantly, variation in cortical thickness, as a function of aging, pathological processes, or individual differences, have been shown to correlate with altered neural activity in the same regions (Hirano et al., 2020; Moretti et al., 2013; Muthukumaraswamy et al., 2010; Palaniyappan et al., 2012; van Pelt et al., 2018). Though previous research has demonstrated the interrelated nature of healthy aging, decreased cortical thickness, and alterations in neural activity, the relationship between these variables has yet to be thoroughly investigated, and this is especially true for the visual cortex.

To date, the majority of aging studies investigating visual cortical responses have demonstrated significant changes in the characteristics of these responses. Most notably, studies using electroencephalography (EEG) and magnetoencephalography (MEG) have shown that

* Corresponding author at: Patrick E. Brookhouser Endowed Chair in Cognitive Neuroscience, Institute for Human Neuroscience, Boys Town National Research Hospital, Boys Town, NE, USA
E-mail address: tony.wilson@boystown.org (T.W. Wilson).

https://doi.org/10.1016/j.neuroimage.2023.120020.
Received 29 November 2022; Received in revised form 21 February 2023; Accepted 10 March 2023
Available online 12 March 2023.

electrode/sensor level responses to visual stimulation in older adults tend to have lower amplitudes (Armstrong et al., 1991a; Kavcic et al., 2013; Polich, 1997; Störmer et al., 2013) and greater latencies compared to those observed in younger individuals (Armstrong et al., 1991a, b; Celesia and Daly, 1977; Kavcic et al., 2013; Price et al., 2017; Sokol et al., 1981; Stephen et al., 2010). While these findings of decreased visual response amplitudes and increased latencies are robust in the electrophysiological literature (e.g., EEG and MEG), studies using functional MRI (fMRI) have been less consistent with some studies supporting the EEG/MEG findings (Cliff et al., 2013; Peiffer et al., 2009; Tekes et al., 2005; West et al., 2019) and many others finding no changes in visual response characteristics as a function of healthy aging (Aizenstein et al., 2004; Brodtmann et al., 2003; Grinband et al., 2017). These discrepancies could be partially attributable to differences in spatial scales, as the EEG and MEG studies that have consistently found age-related effects in visual responses are generally those that relied on sensor/electrode level analyses, which typically reflect responses over more widespread brain regions than is the case with fMRI and source-resolved MEG/EEG. Thus, the anatomical origins of these aging effects and their relationship to observations from fMRI remain poorly understood.

While visual entrainment paradigms have been used in clinical neuroscience research for over 20 years, interest has sharply increased recently due to new evidence suggesting that such entrainment may attenuate beta amyloid plaques in mouse models of Alzheimer's disease (AD) and thus may hold significant therapeutic promise via the capacity to reduce a key pathological feature of the disease (Adaikkan et al., 2019; Iaccarino et al., 2016; Martorell et al., 2019). Visual entrainment responses are generated when neurons in the visual cortices synchronize their firing with the frequency of a flickering visual stimulus. This visual response is unique, relative to non-flickering stimuli, as the neuronal activity is both time- and phase-locked to the visual stimulation and often exhibits an extended duration that matches that of the visual stimulation (Herrmann, 2001; Tsoneva et al., 2021). The use of sustained entrainment paradigms is ideal for investigating visual processing because the elicited neural responses have high signal-to-noise ratios and the sustained nature of the response allows for time varying analysis of visual activity. Nonetheless, despite these advantages, most studies of visual processing in aging have used more simple tasks that involve transient flashes or similar stimuli and focused on the resulting evoke fields (MEG) or potentials (EEG). As briefly mentioned above, beyond aging and recent work in AD, visual (and auditory) entrainment paradigms have been widely used in clinical neuroscience and proven to be useful in the characterization of psychiatric and other neurological disorders (e.g., schizophrenia, autism, ADHD, and migraines; Angelini et al., 2004; Clementz et al., 2004; Jin et al., 2000; Shibata et al., 2008; Wilson et al., 2008; Wilson et al., 2007; Wilson et al., 2012). Further, some of these studies suggest that specific conditions like schizophrenia are associated with deficits in both visual (Clementz et al., 2004; Jin et al., 2000) and auditory domains (Teale et al., 2008; Wilson et al., 2008). However, beyond schizophrenia, the pattern is more unclear because less work has been performed. Interestingly, a recent study also showed that entrainment in one modality (e.g., visual) affects higher order processing of stimuli presented in other modalities (e.g., auditory; Albouy et al., 2022).

In sum, electrode/sensor-level electrophysiological responses serving visual processing using transient, non-flickering visual stimuli have been extensively studied in aging populations, but far less is known about how healthy aging affects cortical-level visual entrainment responses. Further, though cortical thickness changes have been shown to be strongly related to aging, data on the occipital cortex has been less robust and very few studies to date have attempted to link healthy aging to both cortical thinning and visual processing. Thus, in the current study, we examined the neural dynamics of visual entrainment responses using MEG in an aging sample, with an emphasis on neural response amplitude, latency, and consistency (i.e., inter-trial phase-locking and single-trial amplitude consistency). A key goal was to determine whether age-related differences in these response parameters are affected by other functional parameters (e.g., are differences in amplitude attributable to less consistent responses from trial-to-trial) and/or cortical thickness. In order to produce the strongest neural responses, the frequency of entrainment was chosen to fall within the range that has been shown to elicit the most robust visual entrainment responses in healthy adults (i.e., 15 Hz; Pastor et al., 2003). Based on the broader visual processing literature, we hypothesized that, as a function of healthy aging, visual cortical responses would be less consistent, have decreased amplitudes, and increased latencies.

2. Methods and materials

2.1. Participants

A total of eighty adults with a mean age of 46.35 (SD = 13.50) years and a range of 20.22 to 67.00 years were selected for inclusion in this study. These participants were chosen from a larger-scale study of accelerated aging in persons with HIV, with only the HIV-negative participants included in this investigation of healthy aging. Among the included control participants, the number of participants per decade of life was relatively equal (i.e., uniform) and their level of education did not vary as a function of age ($F_{1,77} = 1.91$; $p = .171$). Of the 80 adults, 76 (95%) were right-handed, 63 (79%) were male, 9 (11%) were Black, 5 (6%) were Asian, 63 (79%) were Caucasian, and the remaining 3 (4%) were more than one race, which corresponds closely to the racial demographics of the surrounding region. All participants completed extensive cognitive batteries that assessed the domains of learning, memory, processing speed, attention, executive function, language, and motor function. Following demographic normalization, individual cognitive performance scores were averaged across domains to ensure that each participant scored within the normal range (i.e., within 2 SDs of t-scored values). Exclusionary criteria included any medical illness affecting CNS function (e.g., HIV/AIDS, Lupus, etc.), any neurological or psychiatric disorder, cognitive impairment, history of head trauma, current substance abuse, and the MEG laboratory's standard exclusionary criteria (e.g., ferromagnetic implants). The Institutional Review Board reviewed and approved this investigation. Each participant provided written informed consent following detailed description of the study.

2.2. Experimental paradigm

During the MEG recording, participants sat in a nonmagnetic chair within a magnetically shielded room and were instructed to fixate on an entrainment stimulus that flickered at a rate of 15 times per second (Hz). The stimulus was a small white circle, 3.8 cm in diameter that was presented centrally on a black background and subtended a visual angle of 1.83°. The duration of each flicker-train was 2500 ms and the inter-stimulus interval was randomly jittered between 2000 and 2500 ms. Each participant completed 120 trials, which resulted in a total recording time of about 9.5 min.

2.3. MEG data acquisition

MEG recordings were conducted in a one-layer magnetically shielded room with active shielding engaged to compensate for environmental noise. Neuromagnetic responses were continuously sampled at a rate of 1 kHz with an acquisition bandwidth of 0.1–330 Hz using an Elekta MEG system with 306 magnetic sensors (Helsinki, Finland). During data acquisition, participants were continually monitored via real-time audio-video feeds from inside the magnetically shielded room. MEG data were individually corrected for head motion and subjected to noise reduc-

tion using the signal space separation method with a temporal extension (Taulu and Simola, 2006).

2.4. Structural MRI acquisition, processing, and MEG Coregistration

Preceding MEG recording, four coils were attached to the subject's head and localized, together with the three fiducial points and scalp surface, with a 3-D digitizer (FASTRAK 3SF0002, Polhemus Navigator Sciences, Colchester, VT, USA). Once the participants were positioned for MEG recording, an electric current with a unique frequency label (e.g., 321 Hz) was fed to each of the coils. This induced a measurable magnetic field and allowed each coil to be localized in reference to the sensors throughout the recording session. Since coil locations were also known in head coordinates, all MEG measurements could be transformed into a common coordinate system. With this coordinate system, each participant's MEG data were co-registered with their structural T1-weighted MRI prior to source space analysis using BESA MRI (Version 2.0). Structural MRI data were collected on the same day as the MEG in all but seven participants, with four undergoing MRI within two months of the MEG and three not receiving MRI or having noisy MRI data. For those without high quality MRI data, the MEG data were co-registered to the structural MRI of a demographically similar (i.e., age, sex, weight) participant. Importantly, previous studies have shown that using such a template has a negligible effect on the results (Holliday et al., 2003; Wiesman et al., 2019; Wiesman and Wilson, 2019, 2020) and excluding these participants did not affect our primary neural measures of interest or change any of our significant findings. All MRI data were aligned parallel to the anterior and posterior commissures and transformed into standardized Talairach space. Following source analysis (i.e., beamforming), each subject's 4.0 mm^3 functional MEG images were also transformed into standardized space using the transform that was previously applied to the structural MRI volume and spatially resampled to enable group-wise statistical comparisons.

2.5. MEG preprocessing, time-frequency transformation, and sensor-level statistics

Cardiac and ocular artifacts (e.g., blinks and eye movements) were removed from the data using an adaptive spatial filtering approach which separates artifact and brain signal topographies, allowing for the removal of artifacts without distortion of the underlying neurological signals (Ille et al., 2002). This artifact correction was accounted for during source reconstruction. The continuous magnetic time series was then divided into epochs of 4400 ms duration, with the baseline extending from −600 to 0 ms prior to the onset of the flickering stimulus. Epochs containing remaining artifacts (after cardiac and ocular artifact removal) were rejected, per participant, using a fixed threshold method, supplemented with visual inspection. Across the sample, an average amplitude threshold of 1149.69 (SD = 367.05) fT and an average gradient threshold of 169.69 (94.75) fT/s was used to reject artifacts. An average of 108.15 (SD = 7.66) trials per participant were used for further analysis. Importantly, the amplitude and gradient thresholds used for artifact rejection and the total accepted trial count per participant did not differ as a function of age ($ps > 0.280$).

Artifact-free epochs (−600 to 3800 ms, with zero defined as flicker onset) were then transformed into the time-frequency domain using complex demodulation (Kovach and Gander, 2016), with a time-frequency resolution of 0.5 Hz/100 ms and a bandwidth of 4–50 Hz. The resulting spectral power estimates per sensor were averaged over trials to generate time-frequency plots of mean spectral density per participant. These sensor-level data were then normalized using each respective frequency bin's baseline power, which was derived by averaging over the baseline time window (−600 to 0 ms).

The specific time-frequency windows used for subsequent sourcing imaging were determined by statistical analysis of the sensor-level spectrograms across all trials, gradiometers, and participants. Each data point in the spectrograms were initially evaluated using a mass univariate approached based on the general linear model. To reduce the risk of false-positive results while maintaining reasonable sensitivity, a two-stage procedure was followed to control type 1 error. In the first stage, paired-sample t-tests against baseline were conducted on each data point and the output spectrograms of t-values were thresholded at $p < .05$ to define time-frequency bins containing potentially significant oscillatory deviations across all participants. In stage two, the time-frequency bins that survived the threshold were clustered with temporally and/or spectrally neighboring bins that were also below the threshold ($p < .05$), and a cluster value was derived by summing all of the t-values of all data points in the cluster. Nonparametric permutation testing was then used to derive a distribution of cluster values, and the significance level of the observed clusters (from stage one) were tested directly using this distribution (Ernst, 2004; Maris and Oostenveld, 2007). For each comparison, 10,000 permutations were computed to build a distribution of cluster values. Based on these analyses, the time-frequency windows that contained significant oscillatory events across all participants were subjected to a beamforming analysis. Thus, a data-driven approach was utilized for selecting time-frequency windows to be imaged.

2.6. MEG source imaging and statistics

Cortical networks were imaged through an extension of the linearly constrained minimum variance vector beamformer known as dynamic imaging of coherent sources (Gross et al., 2001), which applies spatial filters to time-frequency sensor data in order to calculate voxel-wise source power for the entire brain volume. Such images are typically referred to as pseudo-t maps, with units (pseudo-*t*) that reflect noise-normalized power differences (i.e., active vs. baseline) per voxel. Following convention, the source power in these images was normalized per participant using a separately averaged pre-stimulus noise period (i.e., baseline) of equal duration and bandwidth (Hillebrand et al., 2005). MEG preprocessing and source imaging used the Brain Electrical Source Analysis (version 7.0) software.

To assess the anatomical basis of the responses identified through the sensor-level analysis, the 3D beamformer output maps were averaged across all participants. To investigate the neural differences in visual processing as a function of healthy aging, virtual sensors (i.e., voxel time series data) were extracted from each participant's MEG data. Specifically, we identified the voxel with the strongest entrainment response in the grand-averaged image (i.e., across all participants and time windows) and computed virtual sensors for that location by applying the sensor weighting matrix derived from the forward solution to the preprocessed signal vector, which yielded a time series for the specific voxel in source space. For this coordinate of interest, the envelope of spectral power was computed for the frequency range used in the beamforming analysis (i.e., 14.5–15.5 Hz, see below). For each participant, the mean baseline activity was derived by averaging the absolute amplitude time series data across the baseline period (−600 to 0 ms). To derive the relative response time series, the absolute amplitude time series was normalized using the same −600 to 0 ms baseline period. Estimates of the relative entrainment response were derived by averaging the relative amplitude time series of the peak voxel across the significant time window derived from the sensor-level data (i.e., 200 to 2600 ms). Further, visual entrainment response latency was determined for each participant by calculating the time it took for them to reach 50% of their maximum entrainment response. Additionally, using these same peak voxel time series, the inter-trial phase locking (ITPL) value was computed per participant for the time-frequency range used in the beamforming analysis (i.e., 14.5–15.5 Hz; 200 to 2600 ms) to assess phase consistency. Finally, to evaluate the consistency of visual entrainment amplitudes across trials, the coefficient of variation was calculated across the single-trial responses for each participant. To reduce the impact of outliers on statistical analyses, participants with values 2.5 SDs above or below the group mean were excluded for each analysis.

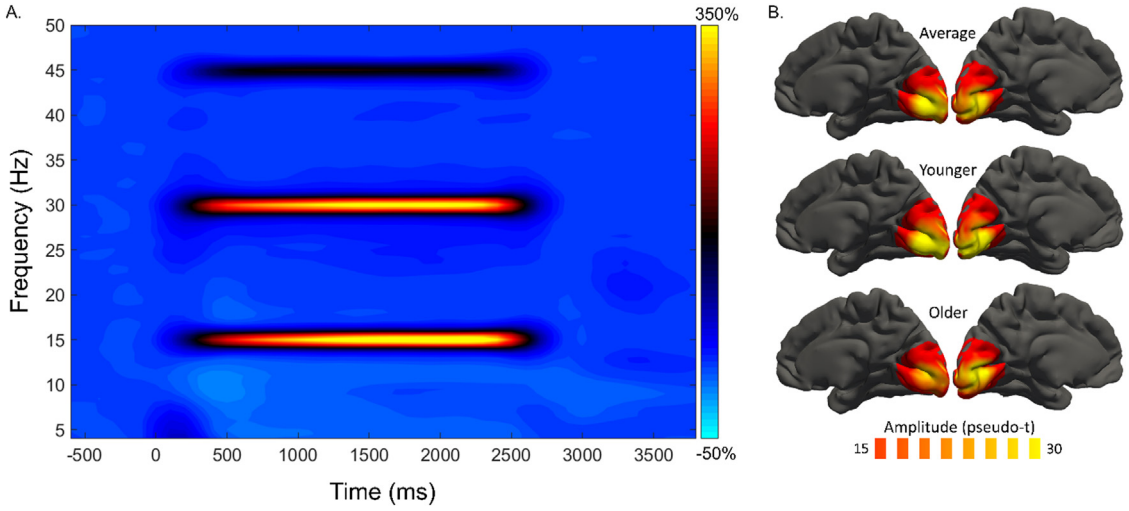

Fig. 1. Sensor- and source-level activity during visual entrainment. A. Grand-averaged time-frequency spectrogram from a sensor near the occipital cortex (i.e., MEG2123), with time (ms) shown on the x-axis and frequency (Hz) denoted on the y-axis. A color scale bar shown to the right of the spectrogram denotes the percent power change relative to the baseline period (−600 to 0 ms). There is clear entrainment to the 15 Hz flicker stimulus and harmonics (i.e., 30 and 45 Hz). **B.** Mean beamformer images (pseudo-*t*; see color bar) of the 15 Hz entrainment response (i.e., 200–2600 ms and 14.5–15.5 Hz). The images labeled "younger" and "older" represent the average source representations for the youngest and oldest participants, as determined with cutoffs of less than or greater than 0.5 standard deviations from the mean age, respectively. Note that all statistical analyses treated age as a continuous variable and the subgroups here are just for illustration purposes.

2.7. Cortical thickness processing

To examine cortical thickness, the T1-weighted MRI data were then processed using additional surface-based morphometry calculations in the computational anatomy toolbox (CAT12 v12.6; Gaser et al., 2022) at a resolution of 1 mm^3. This method uses a projection-based thickness approach to estimate cortical thickness and reconstruct the central surface in one step (Dahnke et al., 2013). Briefly, following tissue segmentation, the white matter distance is estimated, and the local maxima are projected onto other gray matter voxels using a neighboring relationship described by the WM distance. This method accounts for partial volume correction, sulcal blurring, and sulcal asymmetries. Topological defects are corrected based on spherical harmonics (Yotter et al., 2011a) and the cortical surface mesh was reparametrized into a common coordinate system via an algorithm that reduces area distortion (Yotter et al., 2011b). Finally, the resulting maps were resampled and smoothed using a 15 mm FWHM Gaussian kernel. These cortical thickness maps were then parcellated using the Desikan-Killiany (DK) atlas. Subject-wise cortical thickness values were extracted in several ways: 1) averaged across all atlas regions (i.e., entire cortex), 2) averaged across occipital atlas regions (i.e., lingual, pericalcarine, lateral occipital, and cuneus), and 3) primary visual cortex only (i.e., V1; bilateral pericalcarine regions). The three participants without high quality structural MRI data were excluded from these analyses.

2.8. Statistical analyses

All statistical analyses were performed using *R* (R Core Team, 2020), and data plots were generated using *ggplot2* (Wickham, 2016). In order to perform the mediation analysis, the PROCESS macro (Hayes, 2013) for *R* was utilized, with indirect effects estimated using bootstrapping (Preacher and Hayes, 2004). Linear regression analyses were used to test for differences as a function of healthy aging in mean baseline amplitude, relative entrainment amplitude, response latency, average inter-trial phase locking, average entrainment amplitude variability (coefficient of variation), and cortical thickness (i.e., across the entire cortex, occipital cortex, and pericalcarine region). To ensure that age-related changes in occipital cortex and pericalcarine cortical thickness were not responsible for age-related changes in visual entrainment response metrics, linear regression analyses were used to model the relationship between cortical thickness and the visual response metrics. Additionally, inclusion of these cortical thickness measures as nuisance covariates in all reported statistical models did not change the significance or interpretations of any results. Finally, permutation testing of the relative entrainment time series was performed using custom MATLAB scripts (Mathworks, 2018).

3. Results

3.1. Cortical thickness analysis

As detailed in the methods section, cortical thickness estimates were parcellated using the DK atlas. Subject-wise cortical thickness values were then averaged across the entire cortex, the bilateral occipital cortices (i.e., lingual, pericalcarine, lateral occipital, and cuneus), and the bilateral pericalcarine regions. We found significant age-related decreases in cortical thickness across the entire cortex ($F_{1,74}$ = 10.53, p = .002), bilateral occipital cortex ($F_{1,74}$ = 5.81, p = .018), and pericalcarine regions ($F_{1,74}$ = 8.74, p = .004).

3.2. Sensor-level analysis

Sensor-level time-frequency analysis across all participants revealed significant oscillatory responses in a large number of posterior sensors at the base entrainment frequency (i.e., 15 Hz) and harmonics (i.e., 30 and 45 Hz), all of which were increases in amplitude relative to baseline (Fig. 1A). Given the goals of the study, we focused on the base-frequency entrainment response at 15 Hz, which began at about 200 ms after the presentation of the flickering stimulus and remained significantly different from baseline until tapering off around 100 ms following its removal (i.e., 200–2600 ms; $p < .001$, corrected).

3.3. Beamformer and virtual sensor analysis

To determine the cortical origins of the base-frequency entrainment response, we imaged the significant sensor-level time-frequency bin (i.e., 200–2600 ms and 14.5–15.5 Hz) in each participant using a frequency-resolved beamformer. Since our baseline was only 600 ms in duration, we used four non-overlapping time windows to image the full 200–2600 ms response and then averaged these four images in each

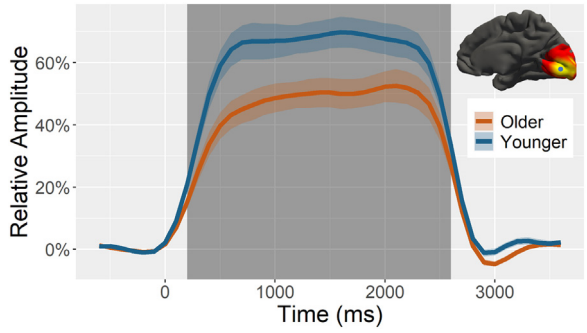

Fig. 2. Relative amplitude of 15 Hz primary visual responses. From the peak voxel exhibiting the strongest neural activity in response to the 15 Hz entrainment stimulus (blue dot within inset image), relative time series (i.e., baseline-corrected) were extracted to evaluate differences in entrainment response amplitude as a function of age during the time window identified through the sensor-level analysis (i.e., 200–2600 ms; shaded area). Note that all statistics treated age as a continuous variable, but for the sake of visualization participants have been dichotomized in this figure using a 0.5 SD from the mean cutoff.

participant. In agreement with previous studies of visual entrainment, strong increases in narrow-band 15 Hz activity were observed in the bilateral primary visual cortices (Fig. 1B). As stated in the methods, we extracted time series data from the peak voxel in the grand-averaged image and then computed the mean relative response amplitude to the flicker stimulus (i.e., 200 to 2600) and the mean absolute amplitude during the baseline period (−600 to 0 ms) to estimate the strength of spontaneous activity. Across the sample, mean entrainment responses became significantly weaker as a function of age ($F_{1,77} = 4.46$, $p = .038$; Figs. 2 and 3A). In contrast, the strength of spontaneous activity during the baseline did not differ as a function of age ($F_{1,77} = 0.04$, $p = .838$; Fig. 3B). Further, mean entrainment responses were not found to be related to visual cortical thickness (occipital cortex: $F_{1,72} = 2.27$, $p = .137$; pericalcarine region: $F_{1,72} = 1.76$, $p = .189$). Note that for these analyses we focused on the two occipital regions since these areas pertain to the origins of the neural responses.

Next, to investigate the temporal dynamics of the entrainment response, we regressed the latency of the response onto participant age (Fig. 3C). We defined the response latency by finding the peak amplitude in each participant and then computing the time it took to reach 50% of that peak in each participant. We found that as age increased, participants took significantly longer on average to entrain to the flickering stimulus ($F_{1,69} = 6.06$, $p = .016$). We then tested for aging effects on the consistency of the entrainment response amplitude using the coefficient of variation (CV) and phase using the ITPL value (Figs. 3D and 3E, respectively). There were no aging effects in the consistency of the cross-trial amplitude ($F_{1,76} = 3.22$, $p = .077$) nor phase ($F_{1,78} = 1.05$, $p = .309$). Further, there was no significant relationship between visual cortical thickness and latency (occipital cortex: $F_{1,66} = 2.75$, $p = .102$; pericalcarine region: $F_{1,66} = 1.89$, $p = .174$), coefficient of variation (occipital cortex: $F_{1,73} = 0.73$, $p = .395$; pericalcarine region: $F_{1,73} = 0.03$, $p = .853$), nor ITPL value (occipital cortex: $F_{1,74} = 0.65$, $p = .423$; pericalcarine region: $F_{1,74} = 0.34$, $p = .564$).

Finally, we wanted to investigate the relationship between response latency and mean entrainment response amplitude, as well as whether latency modulates the relationship between participant age and mean entrainment response. To this end, we regressed the mean entrainment response amplitude onto latency and found that participants with later response latencies (i.e., took longer to entrain to the flickering stimuli) also tended to have weaker mean entrainment responses ($F_{1,69} = 11.60$, $p = .001$). To investigate whether latency mediated the relationship between age and mean entrainment amplitude, a mediation analysis was conducted (Baron and Kenny, 1986), with indirect effects estimated using bootstrapping (Preacher and Hayes, 2004). Our results (Fig. 4 and Table 1) indicated a full mediation of the relationship between age and mean entrainment amplitude by latency, which survived bootstrapping of 5000 samples (95% CI: −.0051 through −.0004). Importantly, these results suggest participant response latency drives the effects of age on the strength of visual entrainment. Further, as with all analyses, the indirect effect of age on mean entrainment amplitude through latency remained significant when controlling for visual cortical thickness.

To further explore these changes in entrainment latency and amplitude as a function of healthy aging, permutation testing of the relative entrainment time series was performed using an initial *p*-value threshold of 0.05 and 10,000 permutations to build the null distribution. Interestingly, of the whole entrainment period (0 to 2500 ms), only the beginning (400 to 1800 ms) differed significantly as a function of age ($p < .05$, corrected). These permutation data provide further support for the idea that changes in the response latency with age may be driving decreases in the overall entrainment amplitudes of older individuals.

4. Discussion

In the current study, we investigated the impact of healthy aging on the visual processing of flickering stimuli in the primary visual cortices while controlling for occipital cortical thickness. Using advanced source reconstruction and voxel time series analyses, we observed robust cortical entrainment at the frequency of stimulation (i.e., 15 Hz) and its harmonics. As expected, as a function of healthy aging, mean entrainment responses were found to decrease in amplitude, while the peak latency of entrainment responses were found to increase. Further, older individuals were found to have decreased cortical thickness across the entire brain and in the visual cortices. These data revealed that entrainment response latency fully mediated the relationship between age and entrainment amplitude, and that these age-related effects surrounded the calcarine fissure. Critically, these changes in visual entrainment response metrics as a function of age were independent of age-related visual cortical thinning. Below, the implications of these novel findings on understanding the impact of healthy aging on visual processing are discussed.

Two common findings in the fMRI and electrode/sensor-level electrophysiologic literature investigating visual processing in healthy aging are decreased amplitude (Armstrong et al., 1991a; Cliff et al., 2013; Kavcic et al., 2013; Peiffer et al., 2009; Polich, 1997; Störmer et al., 2013; Tekes et al., 2005; West et al., 2019) and increased latency (Armstrong et al., 1991a, b; Celesia and Daly, 1977; Kavcic et al., 2013; Price et al., 2017; Sokol et al., 1981; Stephen et al., 2010; West et al., 2019) with increasing age. Our findings support these changes with increasing age predicting weaker visual entrainment and extended time required to fully entrain to the flickering stimulus, and add new anatomical detail on the cortical origins. Broadly speaking, little is known about the underlying cause of such decreased visual response amplitudes in older individuals. In line with the cortical thickness findings in the current study, Peiffer et al. (2009) showed significantly decreased visual response amplitudes even when controlling for visual cortical gray matter loss with increasing age. This research by Peiffer et al. (2009), along with our results showing that visual cortical thinning in older adults is not associated with age-related alterations in visual responses, indicate that age-related changes in visual response properties stem from mechanisms other than the age-related cortical atrophy seen in older individuals. With regards to mechanisms for the increased latency of visual responses with age, however, a fascinating MEG study by Price et al. (2017) demonstrated that prolonged latencies with increasing age could be largely explained by white matter loss in the optic radiations of participants, causing delays in signal transmission.

A secondary goal of the current study was to probe for neurophysiological response parameters that may underlie the decreased visual response amplitudes observed in healthy aging. To this end, we investigated inter-trial phase consistency using the ITPL metric and single trial amplitude using the coefficient of variation (CV), both of which

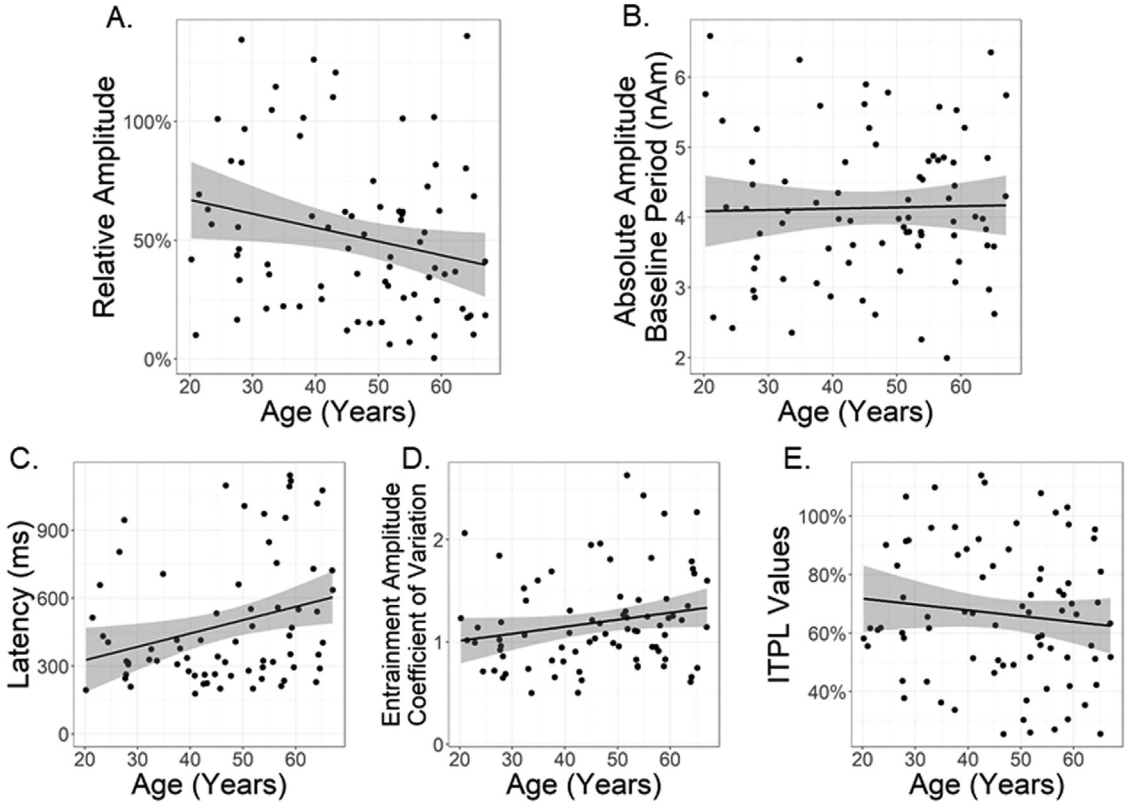

Fig. 3. Relationships between age and several neural indices of the entrainment response. (A) Entrainment response amplitude, (B) Amplitude of spontaneous activity during the baseline period, (C) entrainment response latency, (D) intertrial amplitude consistency (i.e., coefficient of variation), and (E) intertrial phase consistency (i.e., intertrial phase locking; ITPL) are shown as a function of participant age. Lines of linear best-fit, 95% CI (i.e., shaded area).

Table 1
Mediation analysis underlying regressions showing full mediation of the relationship between age and relative entrainment amplitude through latency. $^{*}p < .05$, $^{**}p < .01$.

Model	*b*	*SE*	*t*	*β*	*F*	R^2	95% CI
Simple regression of response latency on age							
Intercept	215.72	117.05	1.84		5.86*	.08	[−17.85, 449.28]
Age	5.81	2.40	2.42*	.282			[1.02, 10.61]
Simple regression of relative entrainment amplitude on age							
Intercept	0.85	0.144	5.90**		5.36*	.07	[0.56, 1.14]
Age	−0.01	0.01	−2.32*	-.270			[−0.01, −0.001]
Multiple regression of relative entrainment amplitude on age and response latency							
Intercept	0.94	0.14	6.68		7.08**	.17	[0.66, 1.22]
Latency	0.00	0.00	−2.87**	-.332			[−0.001, −0.0001]
Age	−0.01	0.00	−1.53	-.177			[−0.01, 0.001]

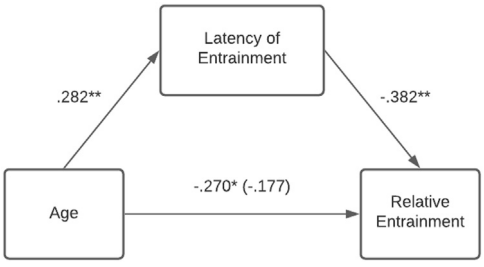

Fig. 4. Mediation analysis revealed that the relationship between age and mean entrainment amplitude was fully mediated by the latency of the entrainment response. This analysis survived bootstrapping of 5000 samples with confidence intervals of 95%. Standardized regression coefficients are displayed. Displayed statistical parameters were not significantly altered when occipital or pericalcarine cortical thickness values were included as nuisance covariates. $^{*}p < .05$, $^{**}p < .01$.

have not been utilized in a healthy aging population. The use of ITPL provides information regarding trial-to-trial phase response consistency that is interpretationally distinct from the coefficient of variation computed on response amplitude across trials. Specifically, ITPL tells us how consistently the phases of the neural signal are aligning from trial to trial (at the same time point) for each participant, while the CV is based on signal amplitude metrics and reflects how consistent the strength of the neural response is from trial to trial. Considering the well documented age-related changes to visual processing, we hypothesized that the consistency of visual responses would decrease with participant age, and thus be a major contributor to the overall decrease in mean amplitude. Interestingly, we observed no such changes in the consistency of the phase (i.e., ITPL) nor amplitude (i.e., CV), which supports the null hypothesis that these parameters do not play a significant role.

A key finding from our time series analyses indicated that older individuals reach their maximum entrainment amplitude much more slowly than their younger peers. This sort of change in response properties has

been shown on a different time scale in fMRI visual processing studies, where older individuals were found to have hemodynamic response curves that were both flatter and more sustained than younger individuals (Aizenstein et al., 2004; West et al., 2019). Similarly, in the current study, visual entrainment response latency was found to predict the mean amplitude of entrainment such that participants who took longer to entrain had weaker overall responses. Thus, to further probe the relationship between age, visual response amplitude, and latency, we conducted a mediation analysis with latency as the mediator. Critically, we found that response latency fully mediated the relationship between age and visual response amplitude, indicating that older individuals may have weaker overall visual responses *because* they are taking longer to entrain the flickering stimuli. This view was fully supported by our permutation analysis of the time series, which showed that older individuals did not statistically differ from younger individuals during the later entrainment period. The fact that older individuals take longer to reach the same visual response amplitude as their younger counterparts is both novel and has important implications for the interpretation of electrophysiologic visual paradigms. In the most common visual stimulation paradigms used in aging research, a stimulus is presented and removed quickly, causing a visual evoked potential. Comparably, entrainment tasks involve quickly flickering the stimulus over and over, which causes a sustained response. The results herein suggest that older participants may have significantly weaker initial visual responses that start to approximate those of their younger peers if the stimulus change is sustained and periodic. Thus, the literature's most common age-related finding in the visual domain may reflect only part of the story, as the decrease in response amplitude is likely paradigm specific.

A somewhat surprising finding was the lack of differences in spontaneous cortical activity as a function of age. Multiple studies have shown elevated spontaneous activity in the primary somatosensory cortices of older adults relative to younger adults (Spooner et al., 2019) and in populations thought to exhibit accelerated aging such as those infected with HIV (Casagrande et al., 2021; Lew et al., 2018; Spooner et al., 2018; Spooner et al., 2020; Wiesman et al., 2018). Likewise, studies have shown elevated spontaneous activity in the primary motor cortices of healthy older relative to younger participants and demonstrated that such activity modulates behavioral performance and oscillatory responses in the same brain tissue (Heinrichs-Graham et al., 2018; Heinrichs-Graham and Wilson, 2016; Rossiter et al., 2014). Thus, we were somewhat surprised that spontaneous activity did not differ as a function of age in the primary visual cortices. One possibility is that such aging effects are limited to the Rolandic region (i.e., extended sensorimotor strip), as we know of no studies showing elevated spontaneous activity with increasing age in the primary auditory or visual cortices. However, a second possibility is that the effect is specific to the idling rhythm of the cortical area, as the motor findings noted above were limited to the beta rhythm. While this is certainly possible, the elevated spontaneous activity reported in the somatosensory cortices of older adults has been limited to the gamma frequency range (Spooner et al., 2019) and the somatosensory strip idles in the alpha band. The primary idling rhythm of the visual cortices is also alpha; thus, future studies should examine whether spontaneous alpha activity is elevated in the primary visual regions of older adults. These studies would ideally involve a task that probes alpha frequency oscillations, as this would enable the impact of elevated spontaneous activity on cognitive and perceptual processing to be determined.

Before closing, it is important to note the limitations of this study. While our sample provided a wide range of ages (i.e., 20.22 to 67.00 years old), the top age was not as old as would have been ideal to cover the entire lifespan (i.e., ~ 80 years old). This is because some research has suggested that the visual declines associated with healthy aging do not significantly worsen until around age 60 (Lachenmayr et al., 1994; Onofrj et al., 2001; Tobimatsu, 1995). Second, the current study only utilized one frequency of stimulation. An interesting future direction would be to expand the frequency of stimulation to several frequencies, particularly those in the gamma band (i.e., > 30 Hz), in order to investigate frequency specific deficits in aging. Finally, despite collecting extensive neuropsychological data, our battery did not include specific assessments of visual processing and future studies of visual entrainment should expand their testing battery in this regard. Despite these limitations, we found that older adults exhibit weaker entrainment responses and that these deficits are largely attributable to older adults reaching peak entrainment much later than younger adults.

Data and code availability statement

The data used in this article will be openly available through the COINS framework (https://coins.trendscenter.org/) once the study is complete. See dataset COINS:PESCAH. Those who wish to use the data can create an account with COINS and complete a data request process for the study, similar to other major open access data repositories.

Credit author statement

Seth Springer: Conceptualization, Methodology, Software, Writing – Original Draft, Writing – Review & Editing, Supervision **Tara Erker**: Formal analysis, Investigation, Writing – Review & Editing, Visualization **Mikki Schantell**: Data Curation **Hallie Johnson**: Project administration, Investigation **Hannah Okelberry**: Project administration, Investigation **Maggie Rempe**: Investigation **Tony Wilson**: Conceptualization, Writing – Review & Editing, Supervision, Project administration, Funding acquisition.

Declaration of Competing Interest

The authors declare that they have no known competing financial interests or personal relationships that could have appeared to influence the work reported in this paper.

Data availability

The data used in this article will be openly available through the COINS framework (https://coins.trendscenter.org/) once the study is complete.

Acknowledgments and funding statement

This research was supported by grants F30-AG076259 (SDS), R01-MH116782 (TWW), R01-MH118013 (TWW), R01-DA047828 (TWW), R01-DA056223 (TWW), RF1-MH117032 (TWW), P20-GM144641 (TWW), and F31-DA056296 (MS) from the National Institutes of Health (NIH). We would like to thank our participants for volunteering in our study.

References

Adaikkan, C., Middleton, S.J., Marco, A., Pao, P.-.C., Mathys, H., Kim, D.N.-W., Gao, F., Young, J.Z., Suk, H.-.J., Boyden, E.S., McHugh, T.J., Tsai, L.-.H., 2019. Gamma entrainment binds higher-order brain regions and offers neuroprotection. Neuron 102, 929–943 e928.

Aizenstein, H.J., Clark, K.A., Butters, M.A., Cochran, J., Stenger, V.A., Meltzer, C.C., Reynolds, C.F., Carter, C.S., 2004. The BOLD hemodynamic response in healthy aging. J. Cogn. Neurosci. 16, 786–793.

Albouy, P., Martinez-Moreno, Z.E., Hoyer, R.S., Zatorre, R.J., Baillet, S., 2022. Supramodality of neural entrainment: rhythmic visual stimulation causally enhances auditory working memory performance. Sci. Adv. 8, eabj9782.

Allen, J.S., Bruss, J., Brown, C.K., Damasio, H., 2005. Normal neuroanatomical variation due to age: the major lobes and a parcellation of the temporal region. Neurobiol. Aging 26, 1279–1282 1245-1260; discussion.

Angelini, L., de Tommaso, M., Guido, M., Hu, K., Ivanov, P., Marinazzo, D., Nardulli, G., Nitti, L., Pellicoro, M., Pierro, C., Stramaglia, S., 2004. Steady-state visual evoked potentials and phase synchronization in migraine patients. Phys. Rev. Lett. 93, 038103.

Armstrong, R.A., Slaven, A., Harding, G.F., 1991a. The influence of age on the pattern and flash visual evoked magnetic response (VEMR). Ophthalmic Physiol. Opt. 11, 71–75.

Armstrong, R.A., Slaven, A., Harding, G.F., 1991b. Visual evoked magnetic fields to flash and pattern in 100 normal subjects. Vision Res. 31, 1859–1864.
Baron, R.M., Kenny, D.A., 1986. The moderator-mediator variable distinction in social psychological research: conceptual, strategic, and statistical considerations. J. Pers. Soc. Psychol. 51, 1173–1182.
Brenner, M.H., Curbow, B., Javitt, J.C., Legro, M.W., Sommer, A., 1993. Vision change and quality of life in the elderly. Response to cataract surgery and treatment of other chronic ocular conditions. Arch. Ophthalmol. 111, 680–685.
Brodtmann, A., Puce, A., Syngeniotis, A., Darby, D., Donnan, G., 2003. The functional magnetic resonance imaging hemodynamic response to faces remains stable until the ninth decade. Neuroimage 20, 520–528.
Burton, K.B., Owsley, C., Sloane, M.E., 1993. Aging and neural spatial contrast sensitivity: photopic vision. Vis. Res. 33, 939–946.
Casagrande, C.C., Lew, B.J., Taylor, B.K., Schantell, M., O'Neill, J., May, P.E., Swindells, S., Wilson, T.W., 2021. Impact of HIV-infection on human somatosensory processing, spontaneous cortical activity, and cortical thickness: a multimodal neuroimaging approach. Hum. Brain Mapp. 42, 2851–2861.
Celesia, G.G., Daly, R.F., 1977. Effects of aging on visual evoked responses. Arch. Neurol. 34, 403–407.
Clementz, B.A., Keil, A., Kissler, J., 2004. Aberrant brain dynamics in schizophrenia: delayed buildup and prolonged decay of the visual steady-state response. Brain Res. Cogn. Brain Res. 18, 121–129.
Cliff, M., Joyce, D.W., Lamar, M., Dannhauser, T., Tracy, D.K., Shergill, S.S., 2013. Aging effects on functional auditory and visual processing using fMRI with variable sensory loading. Cortex 49, 1304–1313.
Dahnke, R., Yotter, R.A., Gaser, C., 2013. Cortical thickness and central surface estimation. Neuroimage 65, 336–348.
Elliott, D., Whitaker, D., MacVeigh, D., 1990. Neural contribution to spatiotemporal contrast sensitivity decline in healthy ageing eyes. Vis. Res. 30, 541–547.
Elliott, D.B., Yang, K.C., Whitaker, D., 1995. Visual acuity changes throughout adulthood in normal, healthy eyes: seeing beyond 6/6. Optom. Vis. Sci. 72, 186–191.
Erdinest, N., London, N., Lavy, I., Morad, Y., Levinger, N., 2021. Vision through healthy aging eyes. Vision (Basel) 5.
Ernst, M.D., 2004. In: Permutation Methods: A Basis for Exact Inference, 19, pp. 676–685.
Fjell, A.M., Westlye, L.T., Amlien, I., Espeseth, T., Reinvang, I., Raz, N., Agartz, I., Salat, D.H., Greve, D.N., Fischl, B., Dale, A.M., Walhovd, K.B., 2009. High consistency of regional cortical thinning in aging across multiple samples. Cereb. Cortex 19, 2001–2012.
Frangou, S., Modabbernia, A., Williams, S.C.R., Papachristou, E., Doucet, G.E., Agartz, I., Aghajani, M., Akudjedu, T.N., Albajes-Eizagirre, A., Alnaes, D., Alpert, K.I., Andersson, M., Andreasen, N.C., Andreassen, O.A., Asherson, P., Banaschewski, T., Bargallo, N., Baumeister, S., Baur-Streubel, R., Bertolino, A., Bonvino, A., Boomsma, D.I., Borgwardt, S., Bourque, J., Brandeis, D., Breier, A., Brodaty, H., Brouwer, R.M., Buitelaar, J.K., Busatto, G.F., Buckner, R.L., Calhoun, V., Canales-Rodríguez, E.J., Cannon, D.M., Caseras, X., Castellanos, F.X., Cervenka, S., Chaim-Avancini, T.M., Ching, C.R.K., Chubar, V., Clark, V.P., Conrod, P., Conzelmann, A., Crespo-Facorro, B., Crivello, F., Crone, E.A., Dale, A.M., Dannlowski, U., Davey, C., de Geus, E.J.C., de Haan, L., de Zubicaray, G.I., den Braber, A., Dickie, E.W., Di Giorgio, A., Doan, N.T., Dørum, E.S., Ehrlich, S., Erk, S., Espeseth, T., Fatouros-Bergman, H., Fisher, S.E., Fouche, J.P., Franke, B., Frodl, T., Fuentes-Claramonte, P., Glahn, D.C., Gotlib, I.H., Grabe, H.J., Grimm, O., Groenewold, N.A., Grotegerd, D., Gruber, O., Gruner, P., Gur, R.E., Gur, R.C., Hahn, T., Harrison, B.J., Hartman, C.A., Hatton, S.N., Heinz, A., Heslenfeld, D.J., Hibar, D.P., Hickie, I.B., Ho, B.C., Hoekstra, P.J., Hohmann, S., Holmes, A.J., Hoogman, M., Hosten, N., Howells, F.M., Hulshoff Pol, H.E., Huyser, C., Jahanshad, N., James, A., Jernigan, T.L., Jiang, J., Jönsson, E.G., Joska, J.A., Kahn, R., Kalnin, A., Kanai, R., Klein, M., Klyushnik, T.P., Koenders, L., Koops, S., Krämer, B., Kuntsi, J., Lagopoulos, J., Lázaro, L., Lebedeva, I., Lee, W.H., Lesch, K.P., Lochner, C., Machielsen, M.W.J., Maingault, S., Martin, N.G., Martínez-Zalacaín, I., Mataix-Cols, D., Mazoyer, B., McDonald, C., McDonald, B.C., McIntosh, A.M., McMahon, K.L., McPhilemy, G., Meinert, S., Menchón, J.M., Medland, S.E., Meyer-Lindenberg, A., Naaijen, J., Najt, P., Nakao, T., Nordvik, J.E., Nyberg, L., Oosterlaan, J., de la Foz, V.O., Paloyelis, Y., Pauli, P., Pergola, G., Pomarol–Clotet, E., Portella, M.J., Potkin, S.G., Radua, J., Reif, A., Rinker, D.A., Roffman, J.L., Rosa, P.G.P., Sacchet, M.D., Sachdev, P.S., Salvador, R., Sánchez-Juan, P., Sarró, S., Satterthwaite, T.D., Saykin, A.J., Serpa, M.H., Schmaal, L., Schnell, K., Schumann, G., Sim, K., Smoller, J.W., Sommer, I., Soriano-Mas, C., Stein, D.J., Strike, L.T., Swagerman, S.C., Tamnes, C.K., Temmingh, H.S., Thomopoulos, S.I., Tomyshev, A.S., Tordesillas-Gutiérrez, D., Trollor, J.N., Turner, J.A., Uhlmann, A., van den Heuvel, O.A., van den Meer, D., van der Wee, N.J.A., van Haren, N.E.M., van 't Ent, D., van Erp, T.G.M., Veer, I.M., Veltman, D.J., Voineskos, A., Völzke, H., Walter, H., Walton, E., Wang, L., Wang, Y., Wassink, T.H., Weber, B., Wen, W., West, J.D., Westlye, L.T., Whalley, H., Wierenga, L.M., Wittfeld, K., Wolf, D.H., Worker, A., Wright, M.J., Yang, K., Yoncheva, Y., Zanetti, M.V., Ziegler, G.C., Thompson, P.M., Dima, D., 2021. Cortical thickness across the lifespan: data from 17,075 healthy individuals aged 3-90 years. Hum. Brain Mapp. 43, 431–451.
Gaser, C., Dahnke, R., Thompson, P.M., Kurth, F., Luders, E., 2022. CAT – A Computational Anatomy Toolbox for the Analysis of Structural MRI Data. Cold Spring Harbor Laboratory.
Griffis, J.C., Burge, W.K., Visscher, K.M., 2016. Age-dependent cortical thinning of peripheral visual field representations in primary visual cortex. Front. Aging Neurosci. 8, 248.
Grinband, J., Steffener, J., Razlighi, Q.R., Stern, Y., 2017. BOLD neurovascular coupling does not change significantly with normal aging. Hum. Brain Mapp. 38, 3538–3551.
Gross, J., Kujala, J., Hamalainen, M., Timmermann, L., Schnitzler, A., Salmelin, R., 2001. Dynamic imaging of coherent sources: studying neural interactions in the human brain. Proc. Natl. Acad. Sci. U. S. A. 98, 694–699.
Hayes, A.F., 2013. Introduction to Mediation, Moderation, and Conditional Process Analysis, 2nd ed. The Guilford Press.
Heinrichs-Graham, E., McDermott, T.J., Mills, M.S., Wiesman, A.I., Wang, Y.P., Stephen, J.M., Calhoun, V.D., Wilson, T.W., 2018. The lifespan trajectory of neural oscillatory activity in the motor system. Dev. Cogn. Neurosci. 30, 159–168.
Heinrichs-Graham, E., Wilson, T.W., 2016. Is an absolute level of cortical beta suppression required for proper movement? Magnetoencephalographic evidence from healthy aging. Neuroimage 134, 514–521.
Herrmann, C.S., 2001. Human EEG responses to 1-100Hz flicker: resonance phenomena in visual cortex and their potential correlation to cognitive phenomena. Exp. Brain Res. 137, 346–353.
Hillebrand, A., Singh, K.D., Holliday, I.E., Furlong, P.L., Barnes, G.R., 2005. A new approach to neuroimaging with magnetoencephalography. Hum. Brain Mapp. 25, 199–211.
Hirano, Y., Oribe, N., Onitsuka, T., Kanba, S., Nestor, P.G., Hosokawa, T., Levin, M., Shenton, M.E., McCarley, R.W., Spencer, K.M., 2020. Auditory cortex volume and gamma oscillation abnormalities in schizophrenia. Clin. EEG Neurosci. 51, 244–251.
Holliday, I.E., Barnes, G.R., Hillebrand, A., Singh, K.D., 2003. Accuracy and applications of group MEG studies using cortical source locations estimated from participants' scalp surfaces. Hum. Brain Mapp. 20, 142–147.
Iaccarino, H.F., Singer, A.C., Martorell, A.J., Rudenko, A., Gao, F., Gillingham, T.Z., Mathys, H., Seo, J., Kritskiy, O., Abdurrob, F., Adaikkan, C., Canter, R.G., Rueda, R., Brown, E.N., Boyden, E.S., Tsai, L.-.H., 2016. Gamma frequency entrainment attenuates amyloid load and modifies microglia. Nature 540, 230–235.
Ille, N., Berg, P., Scherg, M., 2002. Artifact correction of the ongoing EEG using spatial filters based on artifact and brain signal topographies. J. Clin. Neurophysiol. 19, 113–124.
Jin, Y., Castellanos, A., Solis, E.R., Potkin, S.G., 2000. EEG resonant responses in schizophrenia: a photic driving study with improved harmonic resolution. Schizophr. Res. 44, 213–220.
Kavcic, V., Martin, T., Zalar, B., 2013. Aging effects on visual evoked potentials (VEPs) for motion direction discrimination. Int. J. Psychophysiol. 89, 78–87.
Kovach, C.K., Gander, P.E., 2016. The demodulated band transform. J. Neurosci. Methods 261, 135–154.
Lachenmayr, B.J., Kojetinsky, S., Ostermaier, N., Angstwurm, K., Vivell, P.M., Schaumberger, M., 1994. The different effects of aging on normal sensitivity in flicker and light-sense perimetry. Invest. Ophthalmol. Vis. Sci. 35, 2741–2748.
Lew, B.J., McDermott, T.J., Wiesman, A.I., O'Neill, J., Mills, M.S., Robertson, K.R., Fox, H.S., Swindells, S., Wilson, T.W., 2018. Neural dynamics of selective attention deficits in HIV-associated neurocognitive disorder. Neurology 91, e1860–e1869.
Lord, S.R., Dayhew, J., Howland, A., 2002. Multifocal glasses impair edge-contrast sensitivity and depth perception and increase the risk of falls in older people. J. Am. Geriatr. Soc. 50, 1760–1766.
Maris, E., Oostenveld, R., 2007. Nonparametric statistical testing of EEG- and MEG-data. J. Neurosci. Methods 164, 177–190.
Martorell, A.J., Paulson, A.L., Suk, H.-.J., Abdurrob, F., Drummond, G.T., Guan, W., Young, J.Z., Kim, D.N.-W., Kritskiy, O., Barker, S.J., Mangena, V., Prince, S.M., Brown, E.N., Chung, K., Boyden, E.S., Singer, A.C., Tsai, L.-.H., 2019. Multi-sensory gamma stimulation ameliorates Alzheimer's-associated pathology and improves cognition. Cell 177, 256–271 e222.
Mathworks, 2018. MATLAB Natick, Massachusetts, United States.
Moretti, D.V., Paternicò, D., Binetti, G., Zanetti, O., Frisoni, G.B., 2013. EEG upper/low alpha frequency power ratio relates to temporo-parietal brain atrophy and memory performances in mild cognitive impairment. Front. Aging Neurosci. 5, 63.
Muthukumaraswamy, S.D., Singh, K.D., Swettenham, J.B., Jones, D.K., 2010. Visual gamma oscillations and evoked responses: variability, repeatability and structural MRI correlates. Neuroimage 49, 3349–3357.
Onofrj, M., Thomas, A., Iacono, D., D'Andreamatteo, G., Paci, C., 2001. Age-related changes of evoked potentials. Neurophysiol. Clinique/Clin. Neurophysiol. 31, 83–103.
Owsley, C., Ball, K., McGwin, G., Jr., Sloane, M.E., Roenker, D.L., White, M.F., Overley, E.T., 1998. Visual processing impairment and risk of motor vehicle crash among older adults. JAMA 279, 1083–1088.
Palaniyappan, L., Doege, K., Mallikarjun, P., Liddle, E., Francis-Liddle, P., 2012. Cortical thickness and oscillatory phase resetting: a proposed mechanism of salience network dysfunction in schizophrenia. Psychiatriki 23, 117–129.
Pastor, M.A., Artieda, J., Arbizu, J., Valencia, M., Masdeu, J.C., 2003. Human cerebral activation during steady-state visual-evoked responses. J. Neurosci. 23, 11621–11627.
Peiffer, A.M., Hugenschmidt, C.E., Maldjian, J.A., Casanova, R., Srikanth, R., Hayasaka, S., Burdette, J.H., Kraft, R.A., Laurienti, P.J., 2009. Aging and the interaction of sensory cortical function and structure. Hum. Brain Mapp. 30, 228–240.
Polich, J., 1997. EEG and ERP assessment of normal aging. Electroencephalogr. Clin. Neurophysiol./Evoked Potential. Sect. 104, 244–256.
Preacher, K.J., Hayes, A.F., 2004. SPSS and SAS procedures for estimating indirect effects in simple mediation models. Behav. Res. Methods Instrum. Comput. 36, 717–731.
Price, D., Tyler, L.K., Neto Henriques, R., Campbell, K.L., Williams, N., Treder, M.S., Taylor, J.R., Henson, R.N.A., 2017. Age-related delay in visual and auditory evoked responses is mediated by white- and grey-matter differences. Nat. Commun. 8.
R Core Team, 2020. R: A Language and Environment for Statistical Computing. R Foundation for Statistical Computing Vienna, Austria.
Raz, N., Gunning-Dixon, F., Head, D., Rodrigue, K.M., Williamson, A., Acker, J.D., 2004. Aging, sexual dimorphism, and hemispheric asymmetry of the cerebral cortex: replicability of regional differences in volume. Neurobiol. Aging 25, 377–396.
Rossiter, H.E., Davis, E.M., Clark, E.V., Boudrias, M.H., Ward, N.S., 2014. Beta oscillations reflect changes in motor cortex inhibition in healthy ageing. Neuroimage 91, 360–365.

Sakai, H., Uchiyama, Y., Takahara, M., Doi, S., Kubota, F., Yoshimura, T., Tachibana, A., Kurahashi, T., 2015. Is the useful field of view a good predictor of at-fault crash risk in elderly Japanese drivers? Geriatr. Gerontol. Int. 15, 659–665.
Salat, D.H., Buckner, R.L., Snyder, A.Z., Greve, D.N., Desikan, R.S., Busa, E., Morris, J.C., Dale, A.M., Fischl, B., 2004. Thinning of the cerebral cortex in aging. Cereb. Cortex 14, 721–730.
Shibata, K., Yamane, K., Otuka, K., Iwata, M., 2008. Abnormal visual processing in migraine with aura: a study of steady-state visual evoked potentials. J. Neurol. Sci. 271, 119–126.
Sokol, S., Moskowitz, A., Towle, V.L., 1981. Age-related changes in the latency of the visual evoked potential: influence of check size. Electroencephalogr. Clin. Neurophysiol. 51, 559–562.
Spooner, R.K., Wiesman, A.I., Mills, M.S., O'Neill, J., Robertson, K.R., Fox, H.S., Swindells, S., Wilson, T.W., 2018. Aberrant oscillatory dynamics during somatosensory processing in HIV-infected adults. Neuroimage Clin. 20, 85–91.
Spooner, R.K., Wiesman, A.I., O'Neill, J., Schantell, M.D., Fox, H.S., Swindells, S., Wilson, T.W., 2020. Prefrontal gating of sensory input differentiates cognitively impaired and unimpaired aging adults with HIV. Brain Commun. 2.
Spooner, R.K., Wiesman, A.I., Proskovec, A.L., Heinrichs-Graham, E., Wilson, T.W., 2019. Rhythmic spontaneous activity mediates the age-related decline in somatosensory function. Cereb. Cortex 29, 680–688.
Stephen, J.M., Knoefel, J.E., Adair, J., Hart, B., Aine, C.J., 2010. Aging-related changes in auditory and visual integration measured with MEG. Neurosci. Lett. 484, 76–80.
Störmer, V.S., Li, S.-C., Heekeren, H.R., Lindenberger, U., 2013. Normal aging delays and compromises early multifocal visual attention during object tracking. J. Cogn. Neurosci. 25, 188–202.
Taulu, S., Simola, J., 2006. Spatiotemporal signal space separation method for rejecting nearby interference in MEG measurements. Phys. Med. Biol. 51, 1759–1768.
Teale, P., Collins, D., Maharajh, K., Rojas, D.C., Kronberg, E., Reite, M., 2008. Cortical source estimates of gamma band amplitude and phase are different in schizophrenia. Neuroimage 42, 1481–1489.
Tekes, A., Mohamed, M.A., Browner, N.M., Calhoun, V.D., Yousem, D.M., 2005. Effect of age on visuomotor functional MR imaging. Acad. Radiol. 12, 739–745.
Thambisetty, M., Wan, J., Carass, A., An, Y., Prince, J.L., Resnick, S.M., 2010. Longitudinal changes in cortical thickness associated with normal aging. Neuroimage 52, 1215–1223.
Tobimatsu, S., 1995. Aging and pattern visual evoked potentials. Optom. Vis. Sci. 72, 192–197.
Trick, G.L., Silverman, S.E., 1991. Visual sensitivity to motion: age-related changes and deficits in senile dementia of the Alzheimer type. Neurology 41, 1437–1440.
Tsoneva, T., Garcia-Molina, G., Desain, P., 2021. SSVEP phase synchronies and propagation during repetitive visual stimulation at high frequencies. Sci. Rep. 11.
van Pelt, S., Shumskaya, E., Fries, P., 2018. Cortical volume and sex influence visual gamma. Neuroimage 178, 702–712.
West, K.L., Zuppichini, M.D., Turner, M.P., Sivakolundu, D.K., Zhao, Y., Abdelkarim, D., Spence, J.S., Rypma, B., 2019. BOLD hemodynamic response function changes significantly with healthy aging. Neuroimage 188, 198–207.
Wickham, H., 2016. *ggplot2:* Elegant Graphics for Data Analysis. Springer-Verlag, New York.
Wiesman, A.I., Groff, B.R., Wilson, T.W., 2019. Frontoparietal networks mediate the behavioral impact of alpha inhibition in visual cortex. Cereb. Cortex 29, 3505–3513.
Wiesman, A.I., O'Neill, J., Mills, M.S., Robertson, K.R., Fox, H.S., Swindells, S., Wilson, T.W., 2018. Aberrant occipital dynamics differentiate HIV-infected patients with and without cognitive impairment. Brain 141, 1678–1690.
Wiesman, A.I., Wilson, T.W., 2019. Alpha frequency entrainment reduces the effect of visual distractors. J. Cogn. Neurosci. 31, 1392–1403.
Wiesman, A.I., Wilson, T.W., 2020. Posterior alpha and gamma oscillations index divergent and superadditive effects of cognitive interference. Cereb. Cortex 30, 1931–1945.
Wilson, T.W., Hernandez, O.O., Asherin, R.M., Teale, P.D., Reite, M.L., Rojas, D.C., 2008. Cortical gamma generators suggest abnormal auditory circuitry in early-onset psychosis. Cereb. Cortex 18, 371–378.
Wilson, T.W., Rojas, D.C., Reite, M.L., Teale, P.D., Rogers, S.J., 2007. Children and adolescents with autism exhibit reduced MEG steady-state gamma responses. Biol. Psychiatry 62, 192–197.
Wilson, T.W., Wetzel, M.W., White, M.L., Knott, N.L., 2012. Gamma-frequency neuronal activity is diminished in adults with attention-deficit/hyperactivity disorder: a pharmaco-MEG study. J. Psychopharmacol. 26, 771–777.
Yotter, R.A., Dahnke, R., Thompson, P.M., Gaser, C., 2011a. Topological correction of brain surface meshes using spherical harmonics. Hum. Brain Mapp. 32, 1109–1124.
Yotter, R.A., Thompson, P.M., Gaser, C., 2011b. Algorithms to improve the reparameterization of spherical mappings of brain surface meshes. J. Neuroimag. 21, e134–e147.